Influence of Curing Regimes on Engineering and Microstructural Properties of Geopolymer-Based Materials from Water Treatment Residue and Fly Ash

Nguyen Hoc Thang[1], Bui Khac Thach[2], Do Quang Minh[2*]

[1]*Faculty of Chemical Technology, Ho Chi Minh City University of Food Industry, 140 Le Trong Tan Street, Tay Thanh Ward, Tan Phu District, Ho Chi Minh City, 700000, Viet Nam*
[2]*Faculty of Materials Technology, Ho Chi Minh City University of Technology (HCMUT) – Vietnam National University (VNU), 268 Ly Thuong Kiet Street, Ward 14, District 10, Ho Chi Minh City, 700000, Viet Nam*

Abstract. Geopolymerization is a new method for treating water treatment residue (WTR) from water purification plants to reduce the amount of stored land in urban areas. Polymeric bond formation depends on the curing conditions. In this study, the curing conditions suitable for subsequent treatment to save energy consumption and production costs in the future application were investigated. The WTR had a high aluminosilicate content with low alkaline activity, so fly ash (FA) was added to FA and WTR mixtures in the ratio of 40 and 60 weight percent (% in wt.), respectively. The moisture content of the mixtures ranged in 12–15%, suitable for semi-dry pressing to form pellets. After this formation, the geopolymer samples were cured under different conditions (room temperature, microwave oven, in dryer at 110°C, and in autoclave with hydrothermal condition). The experimental results showed that the hydrothermal samples had better properties, such as pH<9, high stability of mechanical strength over 3.5 MPa, and soft coefficient over 0.75. The microstructural properties were investigated using modern analytical tools, such as XRD, SEM, FTIR, and NMR, to detect the chemical functional groups of the aluminosilicate networks in the geopolymer matrix and the close relationship among the properties and its microstructure.

Keywords: Dryer; Fly ash; Geopolymer-based materials; Hydrothermal; Microwave oven; Water treatment residues

1. Introduction

The geopolymerization process involves chemical reactions of aluminosilicates (Al^{3+} with coordinate number 4) with alkaline polysilicate networks for the formation of Si–O–Al bonding (Davidovits, 2020). The geopolymerization products have three-dimensional structural frameworks with the chemical formula as follows:

$$M_n[-(SiO_2)_z-AlO_2]_n.wH_2O$$

where M is the metal cations of K^+, Na^+, Ca^{2+}, and others, n is the degree of condensation, and z = 1, 2, 3, or >> 3. The cations of Na^+, K^+, Ca^{2+}, and others equalize the anions of $[AlO_4]^{5-}$ and $[SiO_4]^{4-}$. The chain and ring structures are formed and networked together based on Si–O–Al sialate bridges (Davidovits, 2020). The geopolymer-based materials were developed based on the new bonding circuits of Q3 and Q4, as known from the reports of

nuclear magnetic resonance (NMR) analyses (Giannopoulou and Panias, 2007; Davidovits, 2020; Rim et al. 2020).

The geopolymer structures are the tetrahedra $[SiO_4]^{4-}$ surrounded by four, three, two, one, or non-tetrahedra $[AlO_4]^{5-}$ (Davidovits, 2020; Rim et al., 2020). The bonding circuit forming units are denoted as Q4(nAl) with n = 0, 1, 2, 3, and 4 corresponding to the number of tetrahedra of $[AlO_4]^{5-}$ or Q represents the $[SiO_4]^{4-}$ tetrahedra. In the ^{29}Si nuclear magnetic resonance spectrum (^{29}Si NMR), Q4(4Al) peaked at 83–88 ppm, Q4(3Al) at 88–94 ppm, Q4(2Al) at 91–98 ppm, Q4(1Al) at 96–105 ppm, and Q4(0Al) at 103–113 ppm (Rim et al. 2020).

Geopolymer-based materials with amorphous phases can transform into crystals known as zeolites when they are supplied suitable energy under known conditions of high temperature and pressure (Zhang et al., 2008). The XRD patterns of geopolymer-based materials with amorphous structural frameworks changed at similar diffraction peaks of zeolite crystals (Davidovits, 2020; Sudibandriyo and Putri, 2020).

Rapid urbanization impedes the use of large land areas to contain water treatment residues (WTR) from water purification plants. Finding new solutions to manage and treat this waste is imperative. Geopolymerization is a new method developed in the last decade to treat waste, such as WTR, from water purification plants (Luukkonen et al., 2019; Numanuddin et al., 2021).

The products based on WTR have very low strength (Waijarean et al., 2013; Geraldo et al., 2017) due to the weak alkaline activity of WTR. Therefore, WTR treatment should be combined with materials of high activity, such as FA (Suksiripattanapong et al., 2015 Horpibulsuk et al., 2016; Janani and Santhi, 2018; Susanto et al., 2020), metakaolin (Geraldo et al., 2017), rice husk ash (Waijarean et al., 2014; Poowancum et al., 2015), and others (Nguyen, 2020a; Nguyen, 2020b; Do et al., 2020a; Do et al., 2020b; Nguyen, 2021, Petrus et al., 2021).

When the samples are cured in an autoclave under high pressure and temperature conditions, the alkaline activators dissolve SiO_2 and Al_2O_3 faster. The H_2O molecules supply $[OH]^-$ to enter into the structures of Na_2O, SiO_2, and Al_2O_3; hence, this is called hydrothermal process. Finally, at atmospheric pressure, the water is removed from the structures to form polymer bonds in the geopolymer-based material by drying (Alas and Ali, 2019; Nguyen, 2021; Nguyen and Dang, 2021; Nguyen et al., 2021a; Nguyen et al., 2021b).

Swanepoel and Strydom (2002) suggested that the optimal condition for strength development of geopolymer samples is at 60°C for 48 h. Palomo et al. (2004) concluded that geopolymer samples based on fly ash (FA) were cured at 65°C for one week or 85°C for 24 h, which had enough energy to achieve levels of reactions and strength responding to the engineering requirements. However, when the temperature was over 60°C, the strength of specimens decreased. Adam and Horianto (2014) revealed that the curing temperature range of 80–120°C for 20 h had better strength than that of curing for 4 and 6 h. The geopolymer-based materials cured in microwave conditions are a new method in a short time from 1 to 7 min. The microwave conditions accelerate the reaction and hardening processes while participating in water elimination reactions (Do et al., 2020a).

The mechanical strength of geopolymer-based materials increases with an increase in alkali concentration from 4 to 10 M (Prasanphan et al., 2019). In the concentration range from 10 to 18 M, the strength of the geopolymer gradually decreased (Alonso and Palomo, 2001). This parallels the experimental results of Mustafa et al. (2012), which revealed increased strength of the geopolymer specimens that used alkali solution from 6–12 M, while the geopolymer samples that used alkali concentration from 12–16 M decreased in strength. The pH values in 13–14 are best for forming geopolymeric networks with good

mechanical properties. The ratios of M_2O/SiO_2, SiO_2/Al_2O_3, H_2O/M_2O, and M_2O/Al_2O_3 (M is Na or K) range from 0.2 to 0.48, 3.3 to 4.5, 10 to 25, and 0.8 to 1.6, respectively (Nguyen, 2020a).

Geopolymers from WTR have many potential applications in building materials, water and wastewater treatment, including adsorbents/ion exchangers, membranes and filter, catalysts, stabilizers of water and WTR (Luukkonen et al., 2019), pH regulators (Novais et al., 2016; Ascensão et al., 2017), and others. The geopolymer materials are considered the materials of the 21st century due to their zero CO_2 emissions in the manufacturing process and their high mechanical strength.

Therefore, in this study, experiments were conducted to produce geopolymer-based materials using industrial solid wastes of WTR and FA. The products were cured under various conditions to determine their engineering properties. Also, the pH values of the geopolymer were tested to assess their impact on the environment. The microstructural properties of the materials were characterized and evaluated using the analytical tools of X-ray diffraction (XRD), Fourier transform infrared spectroscopy (FTIR), scanning electron microscope (SEM), and nuclear magnetic resonance spectroscopy (MNR) to confirm polymeric bond formation in the geopolymer-based material.

2. Materials and Methods

2.1. Specifications of the Raw Materials

This study used WTR from Thu Duc Water Purification Plant, Ho Chi Minh City, and FA was from Vinh Tan 2 Thermal Power Plant in Binh Thuan province, Vietnam. The WTR and FA had average particle sizes of 25.2 µm and 58.6 µm, respectively. Their chemical compositions were analyzed using X ray fluorescence (XRF) (Table 1).

Table 1 Chemical composition (%, in wt.) of raw materials using X ray fluorescence (XRF)

Materials	SiO_2	Al_2O_3	Fe_2O_3	K_2O	Na_2O	CaO	MgO	TiO_2	Others	LOI
WTR	40.09	30.49	9.33	1.00	0.02	0.19	0.10	1.39	0.36	17.03
FA	51.84	24.40	5.64	2.95	0.24	3.46	0.64	1.11	1.15	8.57

2.2. Methodologies

This study used a blend ratio to produce geopolymer samples. Raw materials were mixed in ratios of 6 kg WTR, 4 kg FA, and 0.48 kg NaOH. The amount of water was 15.07% (in weight) and mixed for 15 min using a ball mill. After thorough mixing, the mixture was formed in a roller press. The powder was pressed via roller press to form pellets about 10 mm and 20 mm in diameter and length. The samples were cured in the different curing regimes as follows: ***At room temperatures*** with humidity at 80–85% and temperature of 25–30°C cured for 3, 7, 14, 21, and 28 days to test for engineering and microstructural properties; ***In the dryer*** (Venticell) at temperature of 110°C for 14 h. Then, the samples were cured at room temperature for 3, 7, 14, 21, and 28 days to test for engineering and microstructural properties; ***In a microwave*** (Sanyo EM-S2182W) with a power capacity of 120 W for 5 min. The samples were continuously cured at room temperature for 3, 7, 14, 21, and 28 days to test for engineering and microstructural properties; ***In hydrothermal conditions*** using autoclave equipment at a temperature of 180°C for 8 h. After that, the samples were continuously cured at room temperature for 3, 7, 14, 21, and 28 days to test for engineering and microstructural properties.

The non-deformed geopolymer samples were selected for testing engineering properties, such as compressive strength, soft coefficient, and pH values at curing days of 3,

7, 14, 21, and 28. The pH values were measured daily during the curing time following the standard of ASTM D3987-12 (2020) using the Hanna Instruments HI221 pH meter. The softening coefficient was tested following the Vietnamese standard of TCVN 9362-2012. The geopolymer specimens with the best engineering properties after curing for 28 days were characterized for microstructural properties using FTIR (Thermo ARL ADVANT'X equipment), XRD (Bruker D8 Advanced equipment), SEM (FE-SEM S4800 Hitachi equipment), and NMR (JEOL 400MHz NMR equipment).

3.   Results and Discussion

3.1. Engineering Properties of Geopolymer-based Materials

Figure 1 shows that the geopolymer-based materials changed regarding the volumetric weight of samples during the cured time. The volumetric weight of the autoclave samples decreased continuously from 2.07 to 1.88 g/cm^3 after curing for 28 days. The samples cured in the dryer and microwave oven significantly reduced the volumetric weight for the first 7 days at 1.96 and 1.98 g/cm^3, respectively. After that, their volumetric weights increased over 2.00 g/cm^3 after curing for 28 days. This is related to the absorption of water from the air or the reaction with CO_2 of the free alkali. The experimental results also show that the geopolymer samples cured in hydrothermal conditions using an autoclave had higher stability, uniformity, and quality.
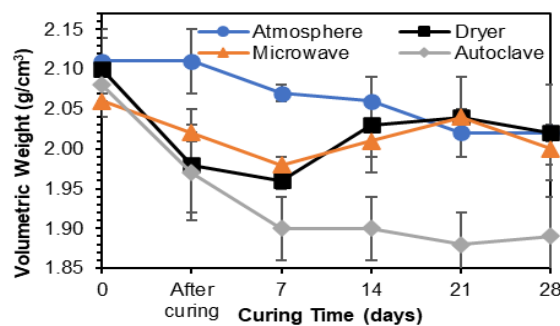

Figure 1 Volumetric weight (g/cm^3) of the samples depending on curing time

The geopolymer samples continuously decreased regarding pH values during the curing time (Figure 2). The samples cured in hydrothermal conditions using autoclave had the lowest pH values of 8.67 for 14 days and 8.88 for 28 days because these samples reacted to the best geopolymerization. However, the pH value gradually decreased in the first days and hardly changed from 21 to 28 days. The decrease in pH is also related to the reaction of CO_2 in the air and water to form H_2CO_3 on the sample surfaces:
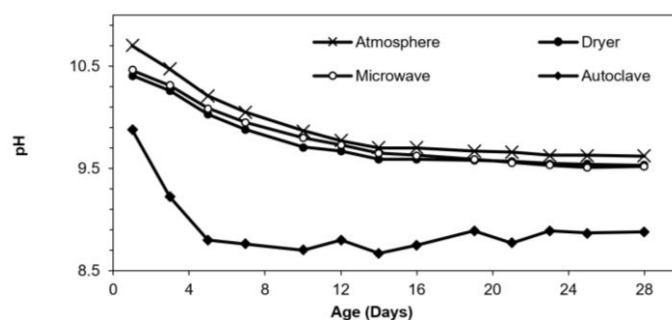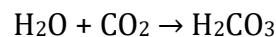
$$H_2O + CO_2 \rightarrow H_2CO_3$$

Figure 2 pH values of the samples depending on curing time

The initial pH of the samples was mainly due to the diffusion of Na^+ ions (Silva et al., 2010). For the samples cured in hydrothermal conditions, the pH value was below that of the samples cured in the other conditions because of the zeolite formation in the hydrothermal reactions. The zeolite kept the Na^+ cations in its structure (Lee et al., 2000).

Figure 3 shows that the geopolymer-based materials changed the compressive strength during the curing time. The compressive strength of samples cured at 28 days significantly exceeded that of the samples cured at 3 and 7 days. The samples cured in the dryer (at a temperature of 110°C for 14 h) after 28 days had the highest compressive strength related to forming a new aluminosilicate structural lattice in the geopolymer-based materials. Notably, the minimum mechanical strength value of the unburned brick is 3.5 MPa, as required in the Vietnamese standard of TCVN 6477-2006.
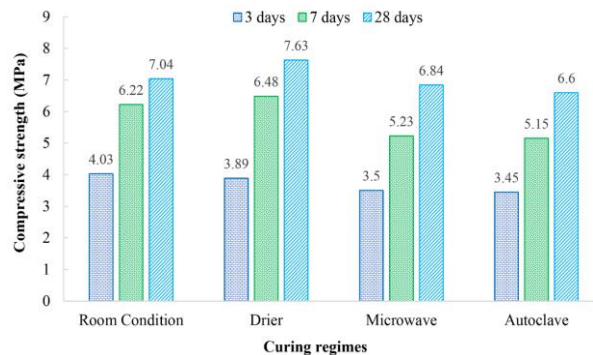

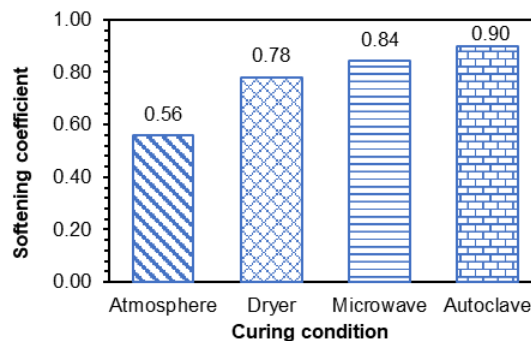**Figure 3** Changes in compressive strength of the geopolymer samples during curing time

Figure 4 Softening coefficient of the samples in the various curing regimes after 28 days

Figure 4 shows the softening coefficient values of the samples. The samples cured at room temperature had the lowest softening coefficient value of 0.56. Other geopolymer samples had softening coefficient values from 0.78 to 0.90, meeting the requirements of the TCVN 9362-2012 Vietnamese standard for unburnt building materials. Notably, the materials had high strength in wet conditions, with the softening coefficient reaching approximately 1.

3.2. Microstructural and Morphological Characteristics of Geopolymer-based Materials

Figure 5 shows the XRD patterns of samples cured in the different conditions compared to the XRD patterns of raw materials (FA and WTR). The XRD patterns of the samples show the amorphous structural features of the aluminosilicate bonding networks in a geopolymeric network matrix. Furthermore, in the narrow range around the diffraction angle of 2-Theta at 26°, there were changes in the diffraction peak intensity of FA and WTR

to form an analcime crystal with 2-Theta at 25.95º and 26.02º, as shown in PDF 00-076-0901.
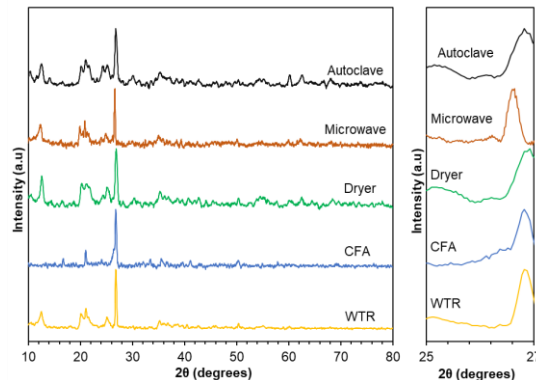

Figure 5 XRD patterns of WTR, FA, and the samples cured in different conditions

This is evident in geopolymer formation (Davidovits, 2020; Nguyen et al., 2020a; Nguyen et al.,2020b; Nguyen, 2021). In addition, crystals such as quartz (SiO_2), kaolinite ($Al_2O_3.2SiO_2.2H_2O$), hematite (Fe_2O_3), and mullite ($3Al_2O_3.2SiO_2$) still exist, as is known in the initial raw materials.

The FTIR spectra in Figure 6 detected asymmetrical elastic oscillation regions of Si–O–T bonding (in which T represents Si or Al) (Panias et al., 2006). This oscillation region is within the wavenumbers from 1100 to 900 cm^{-1} (Schoonheydt et al., 2018; Nguyen et al., 2020b; Nguyen, 2021). The geopolymer formation displaced the absorption peak position of the Si–O–T bonding toward the lower frequency. This is due to the replacement of Al^{3+} ions in the aluminosilicate structural networks (Schoonheydt et al., 2018).

In the wavenumber range of 950–1100 cm^{-1}, there is the displacement of absorption peaks at 1010.52 cm^{-1} and 1033.69 cm^{-1} in the geopolymer samples, and it is below that of reference sample. It is related to the dissolution of the activated SiO_2 and Al_2O_3 from the raw materials into alkaline solution, forming the amorphous structure of the aluminosilicate gel in the geopolymeric network (Lee et al., 2000; Nguyen, 2020a). This is evident for restructuring after the aluminosilicates were dissolved in alkaline solution to form Si–O–Al bonds in the inorganic polymer chains (Davidovits, 2020; Nguyen, 2021).
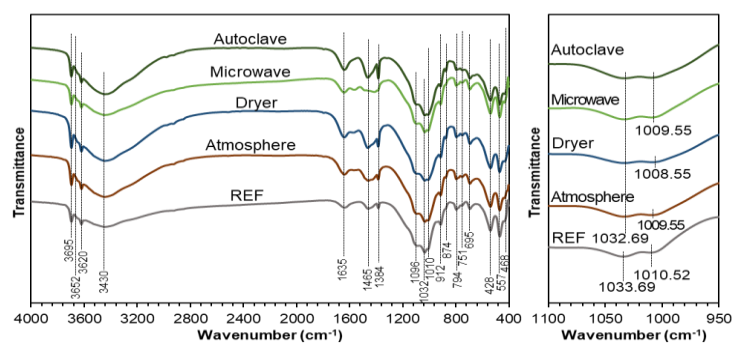

Figure 6 FTIR spectra of the geopolymer samples cured in drier, microwave, and autoclave at room conditions and the FTIR spectrum of the reference geopolymer sample

Two geopolymer samples cured in autoclave and dryer conditions were selected to analyze and evaluate the microstructure and morphological characteristics using SEM (Figure 7). At a magnification of 5000 times, the gel structure of the geopolymer is detected like that of Alehyen et al. (2017). The gel layers appeared more for the samples cured in

autoclave conditions with a better geopolymerization. Besides, the needle-shaped (N) structures are easily detected for the geopolymer cured in the autoclave surrounding FA ball particles. Several pores (P) were formed by the cleavage and dissolution of FA particles. The reacted FA (RFA) and unreacted FA (UFA) are easily seen in SEM images.
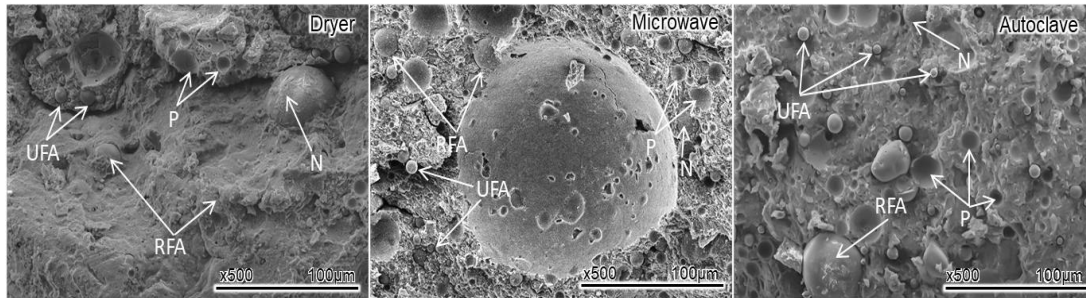

Figure 7 Microstructural and morphologies characteristics of the geopolymer samples cured in drier and autoclave conditions at magnifications of 500 and 5000 times

Figure 8 shows the ^{29}Si NMR spectra of the samples cured in a dryer at 110°C, microwave oven, and hydrothermal conditions after 28 days. The NMR signals at −74.7 ppm (for the sample cured in a microwave oven), −72.6 ppm (for the sample cured in a dryer at 110°C), and −71.2 ppm (for the sample cured in an autoclave) are monosilicate structures corresponding to Q_0 type. The MNR signals at −77.7 ppm (for the sample cured in a microwave oven), −76.4 ppm (for the sample cured in a dryer at 110°C) and −77.6 ppm (for the sample cured in an autoclave) are disilicate or sorosilicate structures or the end of the structural chains corresponding to the Q_1 type (Duxson et al., 2005; Protsak et al., 2019; Rim et al., 2020). The chemical shift from −80 to −100 ppm is related to the $[SiO_4]^{4-}$ tetrahedra surrounded by a different number of $[AlO_4]^{5-}$ tetrahedra (Rim et al., 2020; Duxson et al., 2007). The NMR results are listed in Table 2 with the peaks corresponding to the different structural types in the geopolymeric networks.
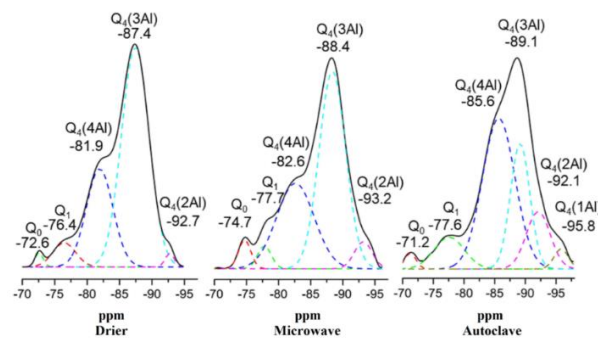

Figure 8 ^{29}Si NMR spectra of the geopolymer samples cured in drier, microwave, and autoclave conditions

Table 2 Summarizes of ^{29}Si NMR signals of the different structural types in geopolymeric networks

Curing regimes	Q_0	Q_1	Q_4(4Al)	Q_4(3Al)	Q_4(2Al)	Q_4(1Al)
Microwave	−74.7	−77.7	−82.6	−88.4	−93.2	-
Dryer	−72.6	−76.4	−81.9	−87.4	−92.7	-
Autoclave	−71.2	−77.6	−85.6	−89.1	−92.1	−95.8

The ^{29}Si NMR spectra clearly showed the formation of $[AlO_4]^{5-}$ in the geopolymer structures of all samples. The sample cured in autoclave conditions had the highest amount of Al^{3+} replacing Si^{4+} in the structures because of the largest region of Q4(4Al), leading to reduced pH values and keeping the alumino-silicate networks in stability.

4. Conclusions

The geopolymer samples were formed through the pressing process of the roller press and cured in various conditions of the drier, microwave, autoclave (hydrothermal), and at room temperature. The results showed that the compressive strength of all samples exceeded 3.5 MPa, responding to the requirements of TCVN 6477-2012 Vietnamese standard. The various curing conditions affected the engineering properties of the geopolymer samples, such as volumetric weight and mechanical strength. The samples cured at room conditions had slow geopolymerization efficiency after 28 days, and they failed for the softening coefficient. The geopolymer samples cured at 110°C using drier and microwave significantly increased in mechanical strength. The samples cured by hydrothermals using autoclaves had high stability on engineering properties and a high-softening coefficient of up to 90%. This demonstrates that geopolymer-based materials have high water resistance when they are cured using the hydrothermal method using autoclave. Moreover, the geopolymer samples cured using the hydrothermal method also had pH values less than 9 because the group of $[AlO_4]^{5-}$ kept the Na^+ cations better than the $[SiO_4]^{4-}$ group based on the results of the ^{29}Si NMR spectrum. Thus, the more Q4(Al) bonds are, the higher the ability to hold Na^+ cations in the aluminosilicate structures of geopolymer. However, the reactions of Na^+ ions with CO_2 filled open pores, increasing the volumetric weight and mechanical strength of the geopolymer samples cured in different conditions. Further research is required to investigate the roles of $[SiO_4]^{4-}$ and $[AlO_4]^{5-}$ in reactions with alkaline activators using the analytical tools of NMR, SEM, FTIR, and XRD.

Acknowledgements

References

Adam, A.A., Horianto, A., 2014. The Effect of Temperature and Duration of Curing on the Strength of Fly Ash Based Geopolymer Mortar. *Procedia Engineering,* Volume 95, pp. 410–414

Alas, M., Ali, S.I.A., 2019. Prediction of the High-Temperature Performance of a Geopolymer Modified Asphalt Binder using Artificial Neural Networks. *International Journal of Technology*, Volume 10(2), pp. 417–427

Alehyen, S., Achouri, M.E., Taibi, M., 2017. Characterization, Microstructure and Properties of Fly Ash-Based Geopolymer. *Journal of Materials and Environmental Science,* Volume 8(5), pp. 1783–1796

Alonso, S., Palomo, A., 2001. Alkaline Activation of Metakaolin and Calcium Hydroxide Mixtures: Influence of Temperature, Activator Concentration and Solids Ratio. *Materials Letter,* Volume 47(1–2), pp. 55–62

Ascensão, G., Seabra, M.P., Aguiar, J.B., Labrincha, J.A., 2017. Red Mud-Based Geopolymers with Tailored Alkali Diffusion Properties and pH Buffering Ability. *Journal of Cleaner Production*, Volume 148, pp. 23–30

Davidovits, J., 2020. *Geopolymer Chemistry and Application.* 5th Edition, Institut
Géopolymère, France

Do, Q.M., Ngo, P.M., Nguyen, H.T., 2020a. Characteristics of a Fly Ash-Based Geopolymer
Cured in Microwave Oven. *Key Engineering Materials,* Volume 850, pp. 63–69

Do, Q.M., Nguyen, V.U.N., Nguyen, H.T., 2020b. Development of Refractory Synthesized from
Waste Ceramic Fiber and Chamotte. *Journal of Polymer & Composites*, Volume 8(2), pp.
101–109

Duxson, P., Fernández-Jiménez, A., Provis, J.L., Lukey, G.C., Palomo, A., van Deventer, J.S.J.,
2007. Geopolymer Technology: The Current State of the Art. *Journal of Materials
Science,* Volume 42(9), pp. 2917–2933

Duxson, P., Provis, J.L., Lukey, G.C., Separovic, F., van Deventer, J.S.J., 2005. ^{29}Si NMR Study
of Structural Ordering in Aluminosilicate Geopolymer Gels. *Langmuir*, Volume 21(7),
pp. 3028–3036

Geraldo, R.H., Fernandes, L.F.R., Camarini, G., 2017. Water Treatment Sludge and Rice Husk
Ash to Sustainable Geopolymer Production. *Journal of Cleaner Production,* Volume 149,
pp. 146–155

Giannopoulou, I., Panias, D., 2007. Structure, Design and Applications of Geopolymeric
Materials. *In:* 3rd International Conference on Deformation Processing and Structure
of Materials, Belgrade, Serbia, pp. 5–15

Horpibulsuk, S., Suksiripattanapong, C., Samingthong, W., Rachan, R., Arulrajah, A., 2016.
Durability Against Wetting–Drying Cycles of Water Treatment Sludge–Fly Ash
Geopolymer and Water Treatment Sludge–Cement and Silty Clay-Cement Systems.
Journal of Material Civil Engineering, Volume 28(1), doi.org/10.1061/(ASCE)MT.1943-
5533.0001351

Janani, S., Santhi, A.S., 2018. Multiple Linear Regression Model for Mechanical Properties
and Impact Resistance of Concrete with Fly Ash and Hooked-End Steel
Fibers. *International Journal of Technology*, Volume 9(3), pp.526–536

Lee, M.G., Yi, G., Ahn, B.J., Roddick, F., 2000. Conversion of Coal Fly Ash into Zeolite and
Heavy Metal Removal Characteristics of the Products. *Korean Journal of Chemical
Engineering,* Volume 17(3), pp. 325–331

Luukkonen, T., Heponiemi, A., Runtti, H., Pesonen, J., Yliniemi, J., Lassi, U., 2019. Application
of Alkali-Activated Materials for Water and Wastewater Treatment: A Review. *Review
in Environmental Science and Biotechnology*, Volume 18, 271–297

Mustafa, A.B.A.M., Kamarudin, H., Hussain, M.B., Rafiza, A.R., Zarina, Y., 2012. Effect of
Na2SiO3/NaOH Ratios and NaOH Molarities on Compressive Strength of Fly-Ash-Based
Geopolymer. *ACI Materials Journal,* Volume 109(5), pp. 503–508

Nguyen, H.T., 2020a. Geopolymerization: A Review on Physico-Chemical Factors Influence
to the Reaction Process. *Journal of Polymer & Composites*, Volume 8(2), pp. 128–137

Nguyen, H.T., 2020b. Novel Porous Refractory Synthesized from Diatomaceous Earth and
Rice Husk Ash. *Journal of Polymer & Composites*, Volume 8(2), pp. 128–137

Nguyen, H.T., 2021. Microstructure Stability and Thermal Resistance of Ash-Based
Geopolymer with Sodium Silicate Solution at High Temperature. *International Journal
of Engineering Research in Africa*, Volume 53, pp. 101–111

Nguyen, H.T., Dang, T.P., 2021. Fly Ash-Based Geopolymer: Green Material in Carbon-
Constrained Society. *Solid State Phenomena*, Volume 321, pp. 65–71

Nguyen, H.T., Dang, T.P., Pham, M.T., Le, V.Q., 2021a. Engineering Properties of Alkali-
Activated Materials Produced from Thu Duc Water Plant Waste Sludge, Fly Ash, and
Alkaline Activator by Semi-dry Pressing Method. *Journal of Polymer & Composites*,
Volume 9(1), pp. 39–48

Nguyen, H.T., Nguyen, V.P., Do, Q.M., 2021b. Effects of Curing Time to Engineering Properties of Alkaline-Activated Materials Synthesized from Thu Duc Water Plant Waste Sludge, Fly Ash, and Geopolymer Aggregate. *Materials Science Forum*, Volume 1029, pp. 111–117

Novais, R.M., Buruberri, L.H., Seabra, M.P., Labrincha, J.A., 2016. Novel Porous Fly-Ash Containing Geopolymer monoliths for Lead Adsorption from Wastewaters. *Journal of Hazardous Materials*, Volume 318, pp. 631–640

Numanuddin M.A., Samarakoon S.M.S.M.K., 2021. Utilization of Industrial By-Products/Waste to Manufacture Geopolymer Cement/Concrete. *Sustainability,* Volume 13(2), ID 873

Palomo, A., Alonso, S., Fernandez-Jiménez, A., Sobrados, I., Sanz, J., 2004. Alkaline Activation of Fly Ashes: NMR Study of the Reaction Products. *Journal of American Ceramic Society,* Volume 87(6), pp. 1141–1145

Panias, D., Giannopoulou, I.P., and Perraki, T., 2006. Effect of Synthesis Parameters on the Mechanical Properties of Fly Ash-Based Geopolymers. *Colloids and Surfaces A: Physicochemical and Engineering Aspects,* Volume 301(1–3), pp. 246–254

Petrus, H.T.B.M., Olvianas, M., Astuti, W., Nurpratama, M.I., 2021. Valorization of Geothermal Silica and Natural Bentonite Through Geopolymerization: A Characterization Study and Response Surface Design. *International Journal of Technology,* Volume 12(1), pp. 195–206

Poowancum, A., Nimwinya, E., Horpibulsuk, S., 2015. Development of Room Temperature Curing Geopolymer from Calcined Water-Treatment-Sludge and Rice Husk Ash. *Calcined Clays for Sustainable Concrete*, Volume 10, pp. 291–297

Prasanphan, S., Wannagon, A., Kobayashi, T., Jiemsirilers, S., 2019. Reaction Mechanisms of Calcined Kaolin Processing Waste-Based Geopolymers in the Presence of Low Alkali Activator Solution. *Construction and Building Materials,* Volume 221, pp. 409–420

Protsak, I.S., Morozov, Y.M., Dong, W., Le, Z., Zhang, D., Henderson, I.M., 2019. A ^{29}Si, ^{1}H, and ^{13}C Solid-State NMR Study on the Surface Species of Various Depolymerized Organosiloxanes at Silica Surface. *Nanoscale Research Letters*, Volume 14(160), pp. 1–15

Rim, G., Marchese, A.K., Stallworth, P., Greenbaum, S.G., Park, A.H.A., 2020. ^{29}Si Solid State MAS NMR Study on Leaching Behaviors and Chemical Stability of Different Mg-silicate Structures for CO_2 Sequestration. *Chemical Engineering Journal,* Volume 396, doi.org/10.1016/j.cej.2020.125204

Schoonheydt, R.A., Johnston, C.T., Bergaya, F., 2018. Clay Minerals and Their Surfaces. *Developments in Clay Science,* Volume 9, pp. 1–21

Silva, I.C.E., Gomes, J.C., Albuquerque, A., 2010. Study of the Structural Stability, pH Variation in Water and Influence of the Curing Conditions on Mechanical Resistance of Mineral Wastes Geopolymeric Artificial Aggregates (WGA) as Alternative Materials for Wastewater Treatment Processes. *Silesian University Technology,* Volume 3, pp. 121–128

Sudibandriyo, M., Putri, F.A., 2020. The Effect of Various Zeolites as an Adsorbent for Bioethanol Purification using a Fixed Bed Adsorption Column. *International Journal of Technology,* Volume 11(7), pp. 1300–1308

Suksiripattanapong, C., Srijumpa, T., Horpibulsuk, S., Sukmak, P., Arulrajah, A., Du, Y.J., 2015. Compressive Strengths of Water Treatment Sludge-Fly Ash Geopolymer at Various Compression Energies. *Lowland Technology International*, Volume 17(3), pp. 147–156

Susanto, H., Fahmi, Y., Hutami, A.T., Hadi, Y.T., 2020. Effects of Fly Ash Loading on the Characteristics of PVC-Based Cation Exchange Membranes for Reverse Electrodialysis. *International Journal of Technology*, Volume 11(3), pp. 544–553

Swanepoel, J.C., Strydom, C.A., 2002. Utilisation of Fly Ash in a Geopolymeric Material. *Applied Geochemistry,* Volume 17(8), pp. 1143–1148

Waijarean, N., Asavapisit, S., Sombatsompop, K., MacKenzie, K.J.D., 2014. The Effect of the Si/Al Ratio on the Properties of Water Treatment Residue (WTR)-Based Geopolymers. *Key Engineering Materials,* Volume 608, pp. 289–294

Waijarean, N., Asavapisit, S., Sombatsompop, K., 2013. Strength and Microstructure of Water Treatment Residue-Based Geopolymers Containing Heavy Metals. *Construction and Building Materials,* Volume 50, pp. 486–491

Zhang, Y., Sun, W., Li, Z., 2008. Infrared Spectroscopy Study of Structural Nature of Geopolymeric Products. *Journal of Wuhan University Technology-Materials Science*, Volume 23(4), pp. 522–527